

Random pinhole attenuator for high-power laser beams

Seong Cheol Park^{1,2}, Hyeok Yun³, Jin Woo Yoon^{1,3}, Seong Ku Lee^{1,3}, Jae Hee Sung^{1,3},

Il Woo Choi^{1,3}, Chang Hee Nam^{1,2} and Kyung Taec Kim^{1,2,*}

¹*Department of Physics and Photon Science, Gwangju Institute of Science and Technology, Gwangju 61005, Korea*

²*Center for Relativistic Laser Science, Institute for Basic Science, Gwangju 61005, Korea*

³*Advanced Photonics Research Institute, Gwangju Institute of Science and Technology, Gwangju 61005, Korea*

Abstract The intensity attenuation of a high-power laser is a frequent task in the measurements of optical science. Laser intensity can be attenuated by inserting an optical element, such as a partial reflector, polarizer, or absorption filter. These devices are, however, not always easily applicable, especially in the case of ultra-high power lasers, because they can alter the characteristics of a laser beam or get easily damaged. In this study, we demonstrated that the intensity of a laser beam could be effectively attenuated using a random pinhole attenuator (RPA), a device with randomly distributed pinholes, without changing beam properties. With this device a multi-PW laser beam was successfully attenuated and the focused beam profile was measured without any alterations of its characteristics. Additionally, it was confirmed that the temporal profile of a laser pulse, including the spectral phase, was preserved. Consequently, the RPA possesses significant potential for a wide range of applications.

Key words: *High power laser; laser diagnostics; intensity attenuation* 2-5 words

*Correspondence to: Kyung Taec Kim, Center for Relativistic Laser Science, Institute for Basic Science, Gwangju 61005, Korea. Email: kyungtaec@gist.ac.kr

I. Introduction

The intensity adjustment of a laser beam is commonly required in optics experiments to avoid the damage of optical components. The intensity of the laser beam can be adjusted using an optical device, such as a partial reflector, polarizing plate, or absorption filter^[1, 2]. In most applications, such a device can be inserted to adjust the intensity of a laser beam^[3]. In some cases the intensity adjustment, however, becomes a challenging task in order not to alter laser characteristics. One example is the beam profile measurement after a plasma mirror used to enhance the temporal contrast of an ultrahigh intensity laser^[4, 5]. Since the plasma mirror works at very high intensity, the laser intensity cannot be attenuated before the plasma mirror. The insertion of a partial reflection mirror without changing the beam alignment cannot be easily done due to the large beam size of such a laser. For example, the 4 PW laser at the Center for Relativistic Laser Science (CoReLS) has the beam size of 30 cm^[6, 7]. It is also difficult to add a polarizing plate or an absorption filter due to optical damage, wavefront deformation and additional dispersion. Consequently, there is a practical need for a new approach capable of adjusting the intensity of a high power laser without modifying the laser characteristics.

As another example, a case of measuring the temporal profile of a laser pulse can be considered. The temporal profile of the laser pulse can be measured using various pulse characterization technique. These techniques rely on nonlinear processes like second harmonic generation or ionization. For example, the tunneling ionization with a perturbation for the time-domain observation of an electric-field (TIPTOE) method rely on the nonlinearity of ionization for the temporal characterization^[8, 9], which is highly sensitive to the intensity of the laser pulse. Thus, it is essential to adjust the intensity of the laser beam precisely. Since devices such as

variable ND filters alter the dispersion condition of the laser pulse, the temporal profile of the laser beam is changed^[10]. Therefore, a new approach for attenuating the intensity of the laser beam is also required.

In this work, we demonstrated the attenuation of laser intensity without changing the properties of a high-power laser beam using a random pinhole attenuator (RPA). The RPA is a board with a large number of randomly distributed pinholes. This kind of device has been utilized for an X-ray beam^[11]. The beam profile of the CoReLS 4 PW laser was measured using the RPA. We demonstrated also the continuous attenuation of laser intensity using the RPA with the gradient in pinhole number density. In addition, the RPA was applied for the temporal characterization of ultrahigh intensity laser pulses because it does not introduce additional dispersion. Since the RPA can be generally used to adjust the intensity of the laser beam, it will be highly useful in many optical applications.

II. Theory of a RPA

A RPA has been designed with the following basic idea. A laser beam with flat-top intensity, characterized by a beam diameter D , is considered to be focused using an ideal lens, as shown in Fig. 1(a). Assuming a constant intensity before the lens, the beam energy is proportional to D^2 and the size of the beam at the focus is proportional to D^{-2} . Thus, the intensity at the focus is proportional to D^4 . In the same way, the intensity of the laser beam, diffracted through a pinhole, is proportional to d^4 . If we introduce N pinholes into this scenario, the strength of the electric field at the focal point would be enhanced by N times, leading to an overall intensity increase of N^2 . Therefore, the attenuation factor of the beam intensity (i.e. the intensity ratio with and without the pinholes) can be obtained as $(N^2 d^4)/D^4$ [12].

It should be noted that this attenuation factor is obtained based on the ordinary Kirchhoff diffraction theory. When the size of the hole becomes comparable to the laser wavelength, other effects such as plasmonic and waveguide effects may arise depending on the material and the thickness of the RPA^[13, 14]. These effects are ignored because the pinhole diameters are much larger than the laser wavelength in this work.

With a sufficiently large number of pinholes, the shape of the focused beam can be maintained as it would be in the absence of pinholes. However, a uniformly distributed array of pinholes results in the appearance of diffracted laser beams on the focal plane, in addition to the laser beam's focus. Other laser beams created by the higher order diffraction can be eliminated by randomizing the distribution of the pinholes. In such setup, all laser beams on the focal plane, with the exception of the 0th-order diffraction, are transformed into noise, thereby avoiding the issue of unwanted diffraction.

Figure 1 provides a simplified illustration of light propagation. The passage of light through a board punctuated by randomly distributed pinholes are illustrated in Fig. 1(a). The calculated light propagation on the yz -plane shown in Fig. 1(a) is shown in Fig. 1(b). We assumed that the laser beam with a diameter of 13 mm is focused using a 1 m focal length ideal lens. The pinhole diameter is 60 μm . The number of the pinhole is 1000. The light diffracted through each pinhole is gathered to a single focal point. Since the optical path lengths from each pinhole to the focus are the same, the beam shape is not changed from the original beam shape. However, their optical path lengths vary depending on the position of the pinhole for the higher order diffractions, their phases are randomized due to the random positions of the pinholes. These beams do not form a well-defined beam, but contribute to the background noise.

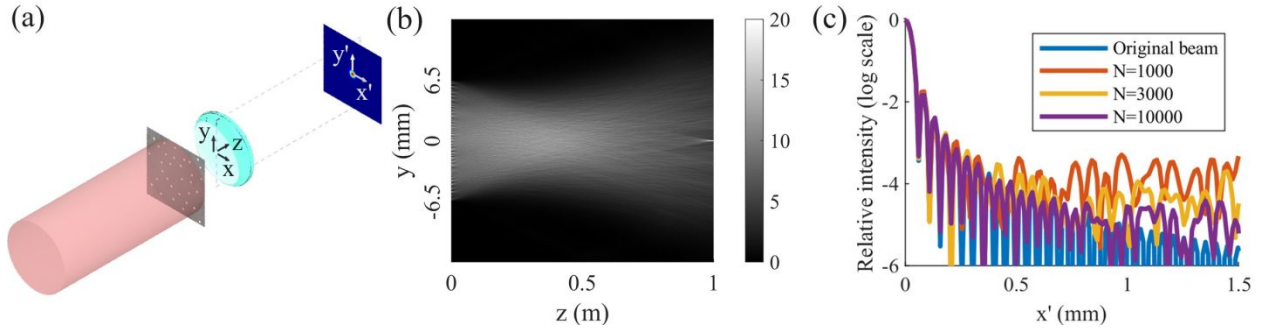


Fig. 1. Attenuation of laser intensity using a random pinhole attenuator (RPA). (a) The schematic diagram for attenuating the laser intensity using the RPA. (b) The intensity of the laser beam on the yz -plane shown in (a). (c) Intensity distribution at the focal plane calculated for different number of pinholes.

To use the RPA, the signal-to-noise ratio (SNR) should be sufficiently high. The energy of the laser beam diffracted through a single pinhole is proportional to d^2 , which is diffracted in an area proportional to $(\lambda f/d)^2$. For the N beams transmitted through the random pinholes, the averaged beam intensity at the focal plane will be proportional to $(Nd^4)/(\lambda f)^2$. Consequently, the noise intensity is proportional to the number of pinhole N while the intensity of the 0th order focused beam is proportional to N^2 . Therefore, the signal-to-noise ratio is proportional to N [15]. The higher the number of pinholes, the higher the signal-to-noise ratio becomes.

We made a series of calculations to estimate the SNR with different number densities of the pinholes, as shown in Fig. 1(c). It is clearly shown that the SNR is enhanced by increasing the number of pinholes for the same beam diameter. Upon calculations with pinhole numbers of 1000, 3000, and 10000, there's a discernible trend of improving SNR with increasing the pinhole numbers.

For an experimental demonstration, a RPA with a density gradient is fabricated by etching holes through a thin metal foil. The pinhole should be randomly distributed with a uniform number density. Also, they must be well separated for fabrication. In order to satisfy these conditions, we used the Poisson disc sampling algorithm^[16, 17]. The density of the pinhole varies from 112 holes/mm² to 11 holes/mm² that corresponds to the optical density (OD) from 2 to 4. Here, the OD value represents the intensity ratio of the laser beam obtained at the focus with and without the random pinhole array. Thus, the OD of 2 means that the beam intensity is reduced to 1/100 of its original value that obtained without the random pinhole array.

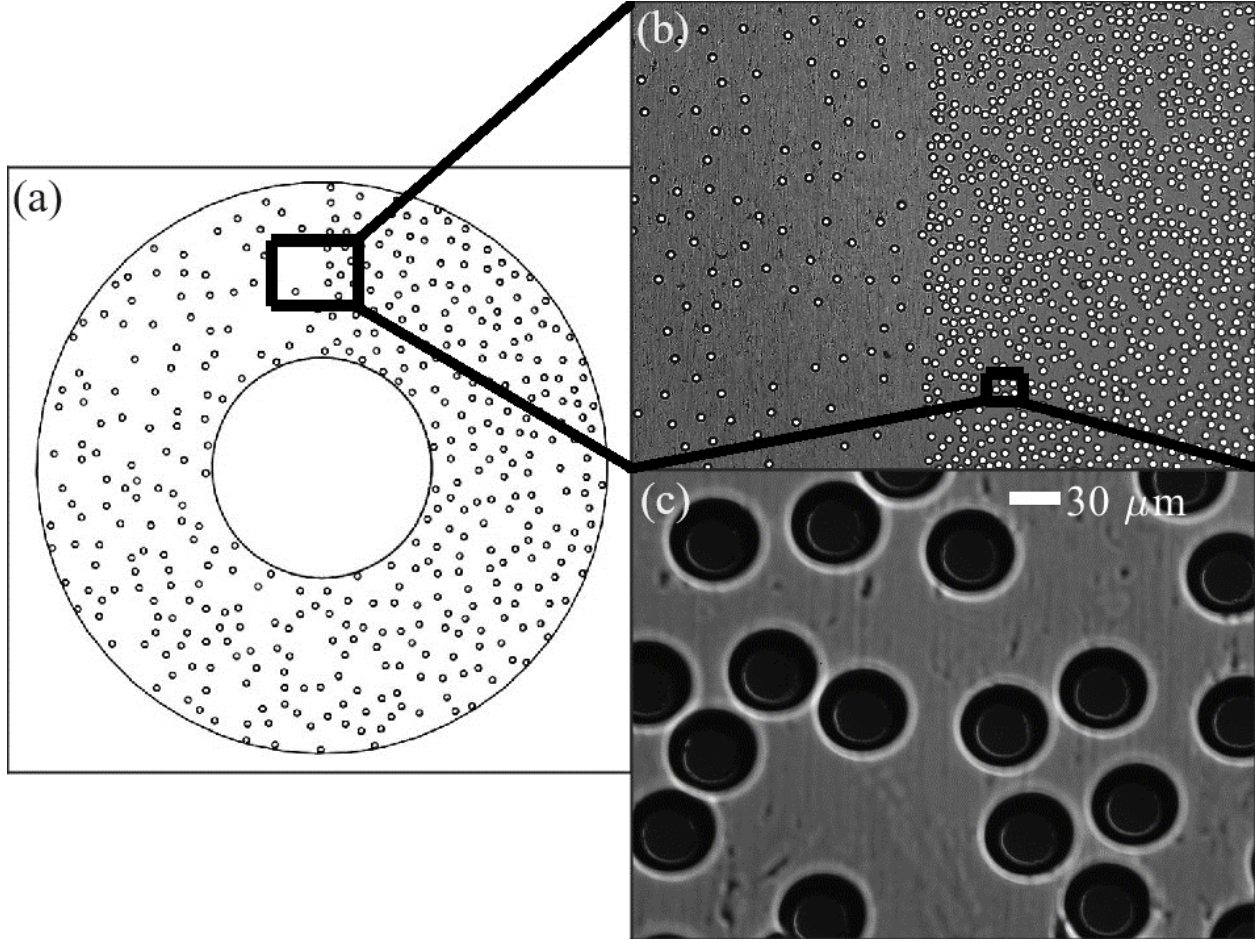


Fig. 2. Random pinhole array fabricated with a number-density gradient. (a) The simplified model of the random pinhole array. (b-c) Microscope images of the random pinhole array obtained with (b) 20x and (c) 50x magnification.

As illustrated in Fig. 2(a), the RPA was designed to adjust the OD values by angle rotation like a commercial variable ND filter (For example, Thorlabs NDC-100C-4M). The number density of the pinholes gradually increases along the peripheral direction. Fig. 2(b) shows an image captured using a 20x magnification microscope lens, which includes both the maximum and minimum densities of holes on the board. Fig. 2(c) employs a 50x magnification microscope lens.

We made circular pinholes. The hole diameter is $30\text{ }\mu\text{m}$. The shape of the pinhole affects the shape of the diffracted beam. However, the focused beam is much smaller than the diffracted beam of the individual pinhole. Therefore, the shape of the individual pinhole is not critical.

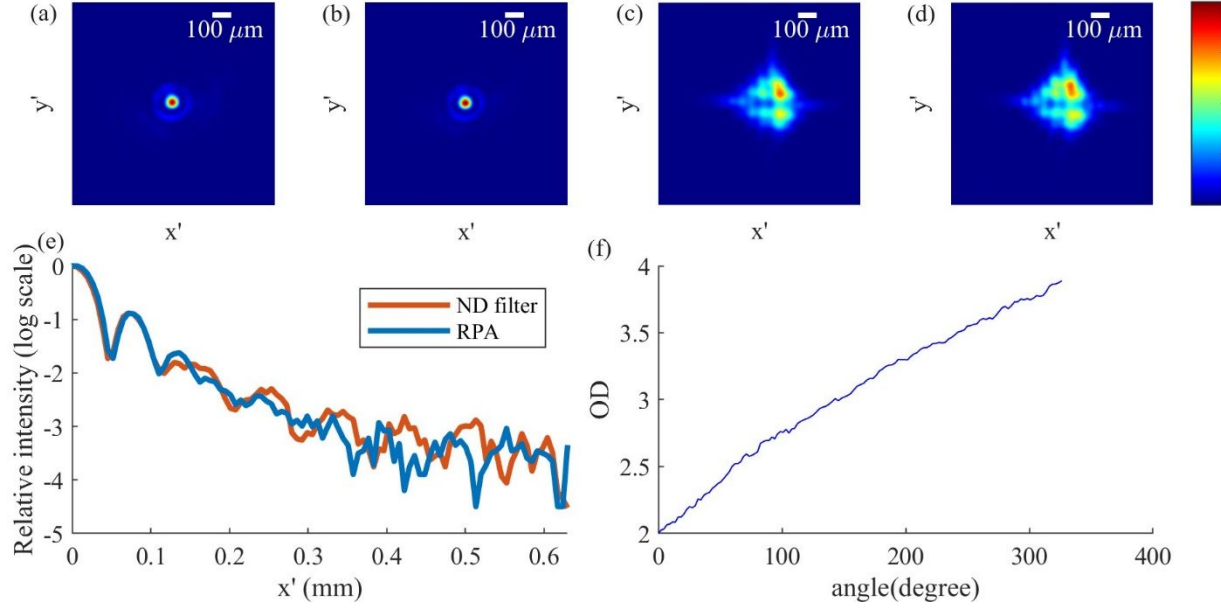


Fig. 3. Beam profiles of the focused beam. (a-d) The beam profiles of the focused beam and the distorted beam. The intensity is attenuated using (a and c) a ND filter (Thorlabs NDC-100C-4M) and (b and d) a RPA. (e) The intensity lineouts along x-axis of the beam shown in (a) and (b). The x-axis represents the distance from the beam's center, while the y-axis depicts the relative intensity on a logarithmic scale. RPA in the legend denotes the RPA. (f) is the measured optical density versus angle of variable attenuation board. OD denotes the optical density.

To verify the idea of a RPA, we first measured the beam profile using a neutral density (ND) filter (THORLABS, NDC-100C-4M), and after then, beam profile was measured using the RPA. A 633 nm diode laser was used for this experiment. A lens with the focal length of 600 mm was utilized to focus the beam, and its profile at the focus was imaged using a CMOS camera (pco.edge 5.5, 16-bit sCMOS camera). The intensity profiles of the laser beam are shown in Fig. 3(a) and 3(b), indicating a good agreement. Consequently, it can be concluded that the beam profile can be measured with the insertion of the random pinhole board. Also, we measured the OD values, showing that the actual OD values varies from 2 to 3.89, as shown in Fig. 3(f). Since the RPA does not change the property of the laser beam, it offers an easy way to control the laser beam intensity.

III. Attenuation of a PW laser beam

To demonstrate the intensity attenuation of a high-power laser beam, we used the CoReLS 4 PW laser. The CoReLS 4 PW laser was operated with an energy of 80 J before the grating compressor. It has been used for various applications such as relativistic high harmonic generation, laser wake field acceleration^[18], and proton acceleration^[19]. In these applications, maintaining an exceptional temporal contrast between prepulses and the main pulse is critical. Therefore, the CoReLS 4 PW laser operates with double plasma mirrors^[20]. It suppresses the intensity of the pre-pulses while the main pulse is reflected with a high reflectance. Since the plasma mirror works when the laser power is sufficiently high, we could not reduce the laser intensity before the plasma mirror. Thus, it was difficult to measure the beam profile of the laser beam at the focus because the conventional techniques to attenuate the beam intensity could not be applied due to the large beam size (30 cm).

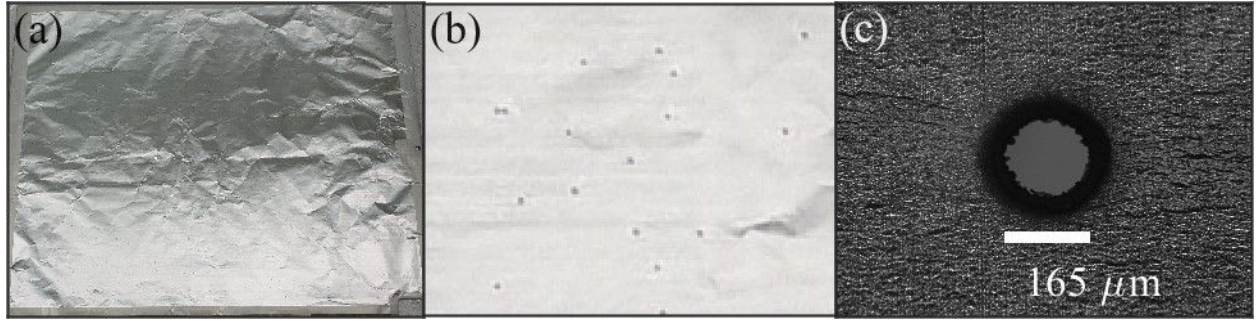


Fig. 4. Photos of a RPA. (a) RPA fabricated on an aluminum foil by laser drilling. (b) Magnified image showing randomly distributed pinholes. (c) Image of a pinhole.

We fabricated a RPA to accommodate the large beam of the CoReLS PW laser as shown in Fig. 4. The detailed parameters of the laser system including the near field beam shape is explained in the Ref^[20]. The random pinhole board was made with 2,500 pinholes with an aperture diameter of 165 μm as shown in Fig. 4(c). These pinholes, distributed randomly within a 300-millimeter circle corresponding to the laser beam's diameter, were fabricated using an aluminum foil whose thickness is 15 μm as shown in Fig. 4(a). The flatness of the foil does not affect to the shape of the focused beam. The pinholes were made by laser drilling using a mJ class, 1 kHz repetition rate, 30 fs pulse duration, 800 nm wavelength Ti:sapphire laser as shown in Fig. 4(b). The energy density of the laser beam that falls on the RPA was 37 mJ/cm² which is well below the damage threshold of the aluminum foil^[21]. No damage was observed after many laser shots.

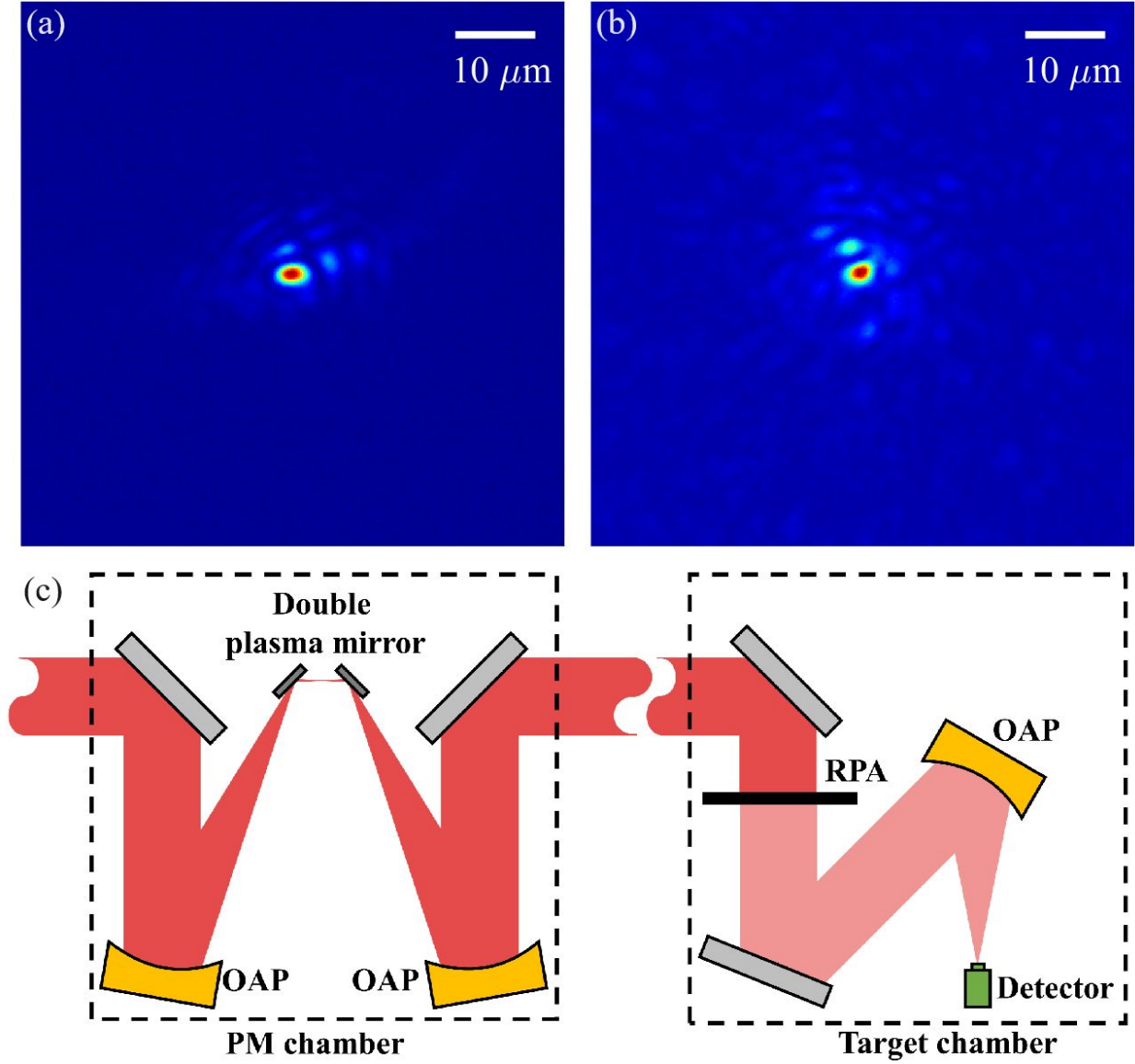


Fig. 5. Beam profiles of the CoReLS 4-PW laser. (a) Beam profile of the focused 10- μJ laser beam without passing through the plasma mirror system, and (b) Beam profile of the focused laser beam obtained with the plasma mirror system. The energy of the laser beam was 80 J before the grating pulse compressor. (c) The schematics of the CoReLS 4-PW laser. The plasma mirrors (PM), RPA, and off axis parabola (OAP) are shown.

The PW laser beam is focused using an off axis parabola with a 550 mm focal length. Since the laser beam intensity is sufficiently reduced, we could measure it directly using an ordinary 12-bit CCD camera as shown in Fig. 5(a) and 5(b). We first measured the beam profile with a commercial ND filter when the laser intensity is weak as shown in Fig. 5(a). We reduced the beam energy down to 4 J. Then, the laser beam is reflected using two 1% reflection mirrors. We also used a waveplate to reduce the laser intensity to 3%. In this case, the plasma mirror was not used. Thus, the laser beam energy was about 10 μ J. Its beam profile is shown in Fig. 5(a).

After that, the laser beam energy was increased to the maximum value (80 J) without having any other attenuation before the plasma mirror. Then, the plasma mirrors were used. The random pinhole board can be positioned at any place in the beam path after the plasma mirror but before the focusing mirror. We placed it about 1 m before the focusing mirror as shown in Fig. 5(c). The beam profile of the laser beam at the focus with the pulse energy of 80 J which is measured before the compressor^[6] is shown in Fig. 5(b).

A noticeable difference exists between the beam profiles in Figs 5(a) and 5(b), attributable to the plasma mirror's deployment. Specifically, in Figure 5(a), the energy insufficiency prevents plasma generation from the mirror, while in Figure 5(b), the laser beam reflects off the plasma given its full energy utilization. An observable non-convergence of the full power beam shown in Fig. 5(b) suggests that the optimization condition of an adaptive optic system (i.e., wavefront sensor and deformable mirror) found for the low intensity beam would not be the best condition for the high-power laser beam.

IV. Attenuation of a laser beam for pulse characterization

The advantage of attenuating the laser beam intensity using the random pinhole board is that it does not alter the property of the laser beam. This is also a great advantage for the temporal characterization of an ultrashort laser pulse. We employed the TIPTOE pulse characterization technique to demonstrate that the laser pulse can be measured without imposing additional dispersion. The temporal profile of the laser beam is measured from the modulation of the ionization yield which is highly sensitive to the laser intensity. Thus, the use of a right intensity is critical in this measurement.

The temporal profiles were measured under two conditions. First, the intensity of the laser beam was attenuated by a commercial variable ND filter (THORLABS, NDC-100C-4M) and the temporal profile of the laser pulse was measured. Then, the temporal profile was also measured using the RPA as shown in Fig. 2. For the latter measurement, a ND filter with the OD of 0.04 was inserted to measure the laser pulse with the same dispersion condition.

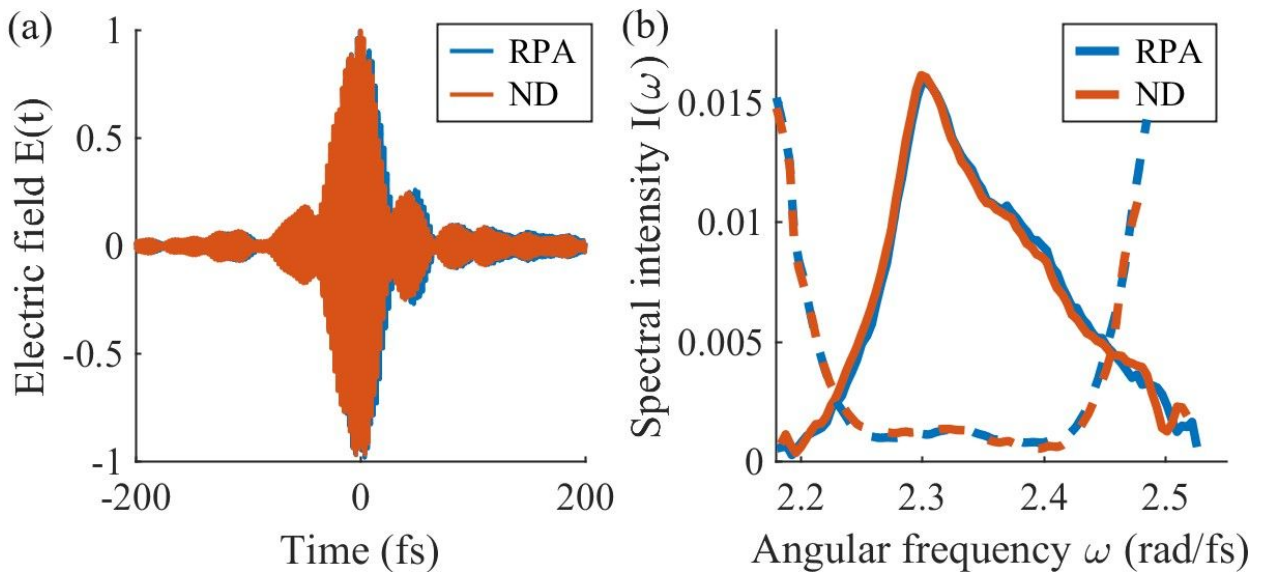


Fig. 6. Comparison of temporal characteristics of two attenuation cases. (a) Laser electric fields obtained with a ND filter (blue line) and with a RPA (red line). (b) Spectral intensities and phases of the two cases.

The temporal profiles are compared in Fig. 6(a). The spectrum and spectral phases are compared in Fig. 6(b). They show a good agreement, indicating that the RPA does not impose any additional dispersion on the laser pulse. It should be noted that the attenuation factor is not dependent on the wavelength. Thus, it can be used for a broadband laser pulse. We also checked the polarization state of the laser beam before and after the RPA. The polarization state was not changed. Therefore, the RPA can be used for the pulse measurement without changing the alignment, polarization, and dispersion condition.

V. Conclusions

We demonstrated the attenuation of laser intensity using a RPA without changing the properties of a high-power laser beam, such as alignment, polarization, and dispersion. Firstly, we provided a theoretical framework illustrating the capability of the RPA. Our calculation showed that the RPA does not significantly alter the beam profile of the focus, which was verified by measuring the beam profile of a diode laser at the focal point. More importantly, we confirmed its usefulness by measuring the beam profile of the CoReLS 4 PW laser, especially after a plasma mirror. In addition, it was verified using the TIPTOE technique that the dispersion condition of a laser beam remained the same after the application of a RPA.

The ability to measure the beam profile of the high power laser system at their full power is critical in many applications. Given the challenges associated with measuring the focus under

full-energy conditions within such systems, our experimental findings mitigate a prevalent uncertainty in application experiments. Importantly, the consistent characteristics of the attenuated beam extend its utility across diverse applications. Since it does not affect to the spatial and temporal property of the laser beam, it will also useful for the measurement of spatio-temporal coupling^[22, 23]. In addition, the RPA can be easily fabricated by chemical etching or laser drilling. Thus, it will be practically useful in many applications.

Acknowledgement

This work was supported by the Institute for Basic Science grant (IBS-R012-D1) and the National Research Foundation of Korea (NRF), grant funded by the Korea government (MIST) (No. 2022R1A2C3006025) and (NRF-2022R1A2C3006025).

References

1. H. A. Macleod, *Thin-Film Optical Filters* (CRC Press, 2017).
2. M. Banning, "Neutral Density Filters of Chromel A1," *JOSA* **37**, 686-687 (1947).
3. C. B. Roundy and K. Kirkham, "Current technology of laser beam profile measurements," *Laser beam shaping*, 463-524 (2014).
4. H. C. Kapteyn, M. M. Murnane, A. Szoke, and R. W. Falcone, "Prepulse energy suppression for high-energy ultrashort pulses using self-induced plasma shuttering," *Optics letters* **16**, 490-492 (1991).
5. A. Lévy, T. Ceccotti, P. D'Oliveira, F. Réau, M. Perdrix, F. Quéré, P. Monot, M. Bougeard, H. Lagadec, and P. Martin, "Double plasma mirror for ultrahigh temporal contrast ultraintense laser pulses," *Optics letters* **32**, 310-312 (2007).
6. J. H. Sung, H. W. Lee, J. Y. Yoo, J. W. Yoon, C. W. Lee, J. M. Yang, Y. J. Son, Y. H. Jang, S. K. Lee, and C. H. Nam, "4.2 PW, 20 fs Ti: sapphire laser at 0.1 Hz," *Optics letters* **42**, 2058-2061 (2017).
7. J. W. Yoon, Y. G. Kim, I. W. Choi, J. H. Sung, H. W. Lee, S. K. Lee, and C. H. Nam, "Realization of laser intensity over 10^{23} W/cm²," *Optica* **8**, 630-635 (2021).
8. S. B. Park, K. Kim, W. Cho, S. I. Hwang, I. Ivanov, C. H. Nam, and K. T. Kim, "Direct sampling of a light wave in air," *Optica* **5**, 402-408 (2018).
9. W. Cho, S. I. Hwang, C. H. Nam, M. R. Bionta, P. Lassonde, B. E. Schmidt, H. Ibrahim, F. Légaré, and K. T. Kim, "Temporal characterization of femtosecond laser pulses using tunneling ionization in the UV, visible, and mid-IR ranges," *Scientific Reports* **9**, 16067 (2019).
10. E. Hecht, *Optics* (Pearson, 2016).
11. J. M. Wengrowicz and G. Hurvitz, "Neutral attenuating pinhole for x-ray imaging of high-intensity sources," *Applied Optics* **59**, 3174-3178 (2020).
12. B. E. Saleh and M. C. Teich, *Fundamentals of photonics* (John Wiley & sons, 2019).
13. H. A. Bethe, "Theory of Diffraction by Small Holes," *Physical Review* **66**, 163-182 (1944).
14. T. W. Ebbesen, H. J. Lezec, H. F. Ghaemi, T. Thio, and P. A. Wolff, "Extraordinary optical transmission through sub-wavelength hole arrays," *Nature* **391**, 667-669 (1998).
15. A. Sommerfeld, *Lectures on theoretical physics: Optics* (Academic press, 1954), Vol. 4.
16. D. Dunbar and G. Humphreys, "A spatial data structure for fast Poisson-disk sample generation," *ACM Transactions on Graphics (TOG)* **25**, 503-508 (2006).
17. R. Bridson, "Fast Poisson disk sampling in arbitrary dimensions," *SIGGRAPH sketches* **10**, 1 (2007).
18. B. S. Rao, J. H. Jeon, H. T. Kim, and C. H. Nam, "Bright muon source driven by GeV electron beams from a compact laser wakefield accelerator," *Plasma Physics and Controlled Fusion* **60**, 095002 (2018).

19. P. Wang, Z. Gong, S. G. Lee, Y. Shou, Y. Geng, C. Jeon, I. J. Kim, H. W. Lee, J. W. Yoon, and J. H. Sung, "Super-heavy ions acceleration driven by ultrashort laser pulses at ultrahigh intensity," *Physical Review X* **11**, 021049 (2021).
20. I. W. Choi, C. Jeon, S. G. Lee, S. Y. Kim, T. Y. Kim, I. J. Kim, H. W. Lee, J. W. Yoon, J. H. Sung, and S. K. Lee, "Highly efficient double plasma mirror producing ultrahigh-contrast multi-petawatt laser pulses," *Optics Letters* **45**, 6342-6345 (2020).
21. S. Xu, Y. Chen, H. Liu, X. Miao, X. Yuan, and X. Jiang, "Femtosecond laser ablation of Ti alloy and Al alloy," *Optik* **212**, 164628 (2020).
22. S. Akturk, X. Gu, P. Bowlan, and R. Trebino, "Spatio-temporal couplings in ultrashort laser pulses," *Journal of Optics* **12**, 093001 (2010).
23. A. Jeandet, S. W. Jolly, A. Borot, B. Bussière, P. Dumont, J. Gautier, O. Gobert, J.-P. Goddet, A. Gonsalves, A. Irman, W. P. Leemans, R. Lopez-Martens, G. Mennerat, K. Nakamura, M. Ouillé, G. Pariente, M. Pittman, T. Püschel, F. Sanson, F. Sylla, C. Thauray, K. Zeil, and F. Quéré, "Survey of spatio-temporal couplings throughout high-power ultrashort lasers," *Opt. Express* **30**, 3262-3288 (2022).